Measurement of an electron's electric dipole moment using Cs atoms trapped in optical lattices

Cheng Chin, Véronique Leiber,* Vladan Vuletić, Andrew J. Kerman, and Steven Chu

Physics Department, Stanford University, Stanford, California 94305-4060

We propose to measure the electron's permanent electric dipole moment (EDM) using cesium atoms trapped in a sparsely populated, trichromatic, far blue-detuned three-dimensional (3D) optical lattice. In the proposed configuration, the atoms can be strongly localized near the nodes of the light field and isolated from each other, leading to a strong suppression of the detrimental effects of atom-atom and atom-field interactions. Three linearly polarized standing waves with different frequencies create an effectively linearly polarized 3D optical lattice and lead to a strong reduction of the tensor light shift, which remains a potential source of systematic error. Other systematics concerning external field instability and gradients and higher-order polarizabilities are discussed. Furthermore, auxiliary atoms can be loaded into the same lattices as effective ''comagnetometers'' to monitor various systematic effects, including magnetic-field fluctuations and imperfect electric-field reversal. We estimate that a sensitivity 100 times higher than the current upper bound for the electron's EDM of $4 \times 10^{-27} e$ cm can be achieved with the proposed technique.

PACS number(s): 32.80.Pj, 11.30.Er, 32.10.Dk, 32.60.+i

I. INTRODUCTION

A permanent electric dipole moment (EDM) for any fundamental particle constitutes a violation of both time-reversal (T) and parity (P) symmetries, and is virtually forbidden in the standard model [1,2]. However, recent supersymmetric theories predict substantially larger T- or P-violating effects, and the corresponding EDMs have been estimated to be within the reach of experiments in the near future [1].

Experimental efforts to detect the EDM of a fundamental particle have concentrated on the neutron and also on ground-state neutral atoms, where T-violating effects from the electron or in the nucleus can manifest themselves as an atomic EDM. Thus far, null results have been obtained within experimental uncertainties. For the neutron and the mercury atom, upper bounds of $6 \times 10^{-26} e$ cm [3] and $8.7 \times 10^{-28} e$ cm [4], respectively, have been established. The current limit on the electron's electric dipole moment of $4 \times 10^{-27} e$ cm was deduced from measurements on a thermal beam of Tl atoms [5]. The present experimental resolution is limited by the large longitudinal velocity of the atomic beam, which not only limits the measurement time, i.e., the time the atoms spend in the interaction region, but also leads to a systematic effect caused by a motion-induced magnetic field [6].

Both effects can be significantly reduced by using optically cooled and trapped atoms. Cooling dramatically decreases the velocity, and therefore the motion-induced magnetic field, while trapping randomizes the direction of motion, which strongly suppresses residual systematic errors when the interrogation time far exceeds the vibration period. Additionally, a long coherence time of several seconds has been demonstrated for optically trapped atoms [7], and even longer coherence times are possible. Even though the atom number and thus the signal-to-noise ratio are reduced in comparison to an atomic beam, this is compensated for by an increase in the measurement time of up to three orders of magnitude. Finally, different atomic species can be loaded into the same far-detuned lattice simultaneously, where the auxiliary atoms trapped in the same volume serve as a co-magnetometer [8] and can be used in real time to investigate and correct for the various potential systematic effects induced by external fields.

However, the interaction between the atoms and the trapping light, as well as enhanced collisions at ultralow temperatures may lead to new limitations that must be carefully investigated. Of special importance are effects that lead to a relative energy shift or decoherence between the magnetic substates, $|F, +m_F\rangle$ and $|F, -m_F\rangle$, where F and m_F denote the hyperfine and magnetic quantum number, respectively, since an electric field-induced energy splitting between these states is the experimental signature for an atomic EDM. For atoms interacting with far-detuned trapping light, the dominant effect of this type is produced in leading order by a circularly polarized component of the light field [9,10], and in higher orders by a third-order interference effect involving both the electric and the magnetic fields of the laser, as well as the static electric field [10]. Atomic collisions can also cause relative energy shifts of different magnetic sublevels as well as spin-relaxation, which can be catastrophic for precision measurements with separated oscillatory fields, as observed in atomic clocks [11].

In this paper, we propose an experimental configuration designed to suppress the detrimental effects of atomic collisions and simultaneously the interaction between the atoms and external fields. This is achieved by confining the atoms in low-lying vibrational states of a three-dimensional (3D) far blue-detuned optical lattice at an average lattice site occupation much smaller than unity (Fig. 1). The lattice is formed by three linearly polarized standing waves, each with a slightly different frequency; the resulting 3D light field has effectively linear polarization throughout space, which is of prime importance for eliminating the leading-order systematic effects caused by the atom–light interaction. Since the

---

*Present address: ENSPS (Ecole Nationale Supérieure de Physique de Strasbourg), Strasbourg, France.
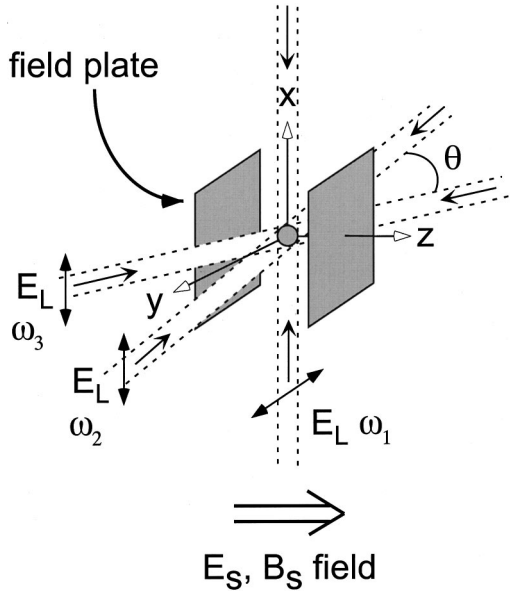
FIG. 1. Proposed experimental configuration. Three standing waves form an optical lattice. They have different frequencies and polarizations that are linear and perpendicular to the quantization axis defined by the external $\mathbf{B_S}$ field and $\mathbf{E_S}$ field. Two horizontal standing waves in the y-z plane intersect with an angle $\theta = 10°$, and are symmetric relative to the y axis.

atoms are localized at the nodes of the blue-detuned light field, these interactions are even further reduced. In this lattice, the atoms can be cooled to the vibrational ground state using Raman sideband cooling [12], and the collision rate between atoms is then limited by the site-to-site tunneling rate, which is exponentially suppressed in the tight-binding regime. Finally, as the position and size of the atomic cloud are defined by the trapping light, systematic effects due to changes in the atomic position in the presence of external forces and field gradients and decoherence due to external field inhomogeneities are greatly reduced.

The electron's EDM d_e is inferred from the magnitude of the atomic EDM d_{atom} [13]. In heavy atoms with a single unpaired electron, a nonzero d_e can induce a permanent ground-state atomic EDM d_{atom} that significantly exceeds d_e. In a perturbative description, the ground state of the atom acquires a dipole moment when it is mixed with higher excited states through the interaction of the electron's EDM with the electric field of the nucleus. In alkali atoms, the largest admixture is from the first excited $P_{1/2}$ and $P_{3/2}$ states, which contribute with opposite sign. Due to the fine structure splitting between these states, the dipole moments induced by the $P_{1/2}$ and $P_{3/2}$ states cancel incompletely and result in a nonzero atomic EDM, $d_{atom} = R d_e$, where R is known as the enhancement factor [13]. Large enhancement factors of $R_{Tl} = -600$ and $R_{Cs} = 114$ have been calculated for the Tl [14] and Cs [15] ground states, respectively, which are both well-suited for measuring the electron's EDM.

An atomic EDM can be detected through its interaction V_{EDM} with an external stationary electric field $\mathbf{E_S}$, $V_{EDM} = -\mathbf{d}_{atom} \cdot \mathbf{E_S} = -R d_e \hat{\mathbf{f}} \cdot \mathbf{E_S}$, where $\hat{\mathbf{f}} \equiv \mathbf{F}/F$, $\mathbf{F} \equiv \mathbf{I} + \mathbf{J}$ is the total angular momentum of the atom, $\mathbf{I}(\mathbf{J})$ is the nuclear

(electronic) angular momentum, and the second equality follows from the Wigner-Eckart theorem. If the quantization axis is chosen along $\mathbf{E_S}$, this interaction results in an energy splitting that depends linearly on $\mathbf{E_S}$ and on the atomic magnetic quantum m_F number associated with the orientation of the total angular momentum $\mathbf{F}$. Observation of a relative energy shift upon reversing the direction of $\mathbf{E_S}$ constitutes a measurement of the electron's EDM $\mathbf{d_e}$.

II. EXPERIMENTAL CONFIGURATION

Our proposed experimental procedure begins by loading the optically precooled cesium atoms into a 3D linearly polarized optical lattice, shown in Fig. 1. Efficient loading and further cooling to the vibrational ground state can be achieved by using Raman-sideband cooling which requires only a small bias magnetic field [12]. After cooling, atoms are optically pumped into the $|F=3, m_F=0\rangle$ state. A coherent superposition of the $|3,2\rangle$, $|3,0\rangle$, and $|3,-2\rangle$ states is then prepared by means of a two-photon Raman transition with $\sigma^{\pm}$ polarized photons. Since the $\sigma^+ - \sigma^-$ transition only couples $|3,0\rangle$ to $|3,\pm2\rangle$, the sample can be treated as a three-level system and 50% populations in $|3,\pm2\rangle$ can be attained by a $\pi/2$ pulse. After evolution in the external electric field ($E_s \sim 10^7$ V/m) for a time T, another Raman pulse is applied that recombines the different magnetic sublevels and is sensitive to the relative phase between $|3,2\rangle$ and $|3,-2\rangle$ accumulated during this time T. The detection of the population in $|3,0\rangle$ as a function of the Raman detuning then constitutes a Ramsey-type measurement of the energy splitting ΔE between the states $m=2$ and $m=-2$. Any change of ΔE upon reversal of the electric field translates into a phase shift over the measurement time T, and is detected as a change of population in the $|3,0\rangle$ state. The populations in different magnetic sublevels can be detected with high sensitivity by first transferring the atoms from $|3,i\rangle$ to $|4,i\rangle$ with a microwave π pulse, and subsequently integrating the fluorescence on the $6S_{1/2}$, $F=4$ to $6P_{3/2}$, $F'=5 \sigma^+$ cycling transition. By repeating this procedure for all three sublevels, we can obtain the populations of all three magnetic sublevels $|3,\pm2\rangle$ and $|3,0\rangle$, which is necessary to normalize the signal and suppress the noise due to shot-to-shot atom number variation.

The EDM induced energy splitting between $|3,2\rangle$ and $|3,-2\rangle$ is expressed as $\Delta E_{EDM} = R d_e E_s$. The projected 100-fold improvement in sensitivity in the measurement of the electron's EDM over that achieved in Ref. [5] requires a frequency sensitivity and total systematic and statistical uncertainty in the d_{Cs} measurement of 100 nHz or better for an electric field of 10^7 V/m. Assuming that single measurements with a coherence time T are performed on samples containing N atoms in the course of a total averaging time t, the Ramsey-type measurement has a shot noise-limited frequency sensitivity of $\Delta\nu = (4\pi^2 NtT)^{-1/2}$ [16–18]. For $N = 10^8$ atoms and $t=8$ h of integration time, we conclude that a coherence time $T \sim 1$ s, and therefore a frequency resolution of $\xi = (4\pi^2 NT)^{-1/2} = 16 \mu$Hz/$\sqrt{\text{Hz}}$ is necessary to reach the envisioned sensitivity. The systematic uncertainty of the energy splitting and the dephasing rate must then be sup-
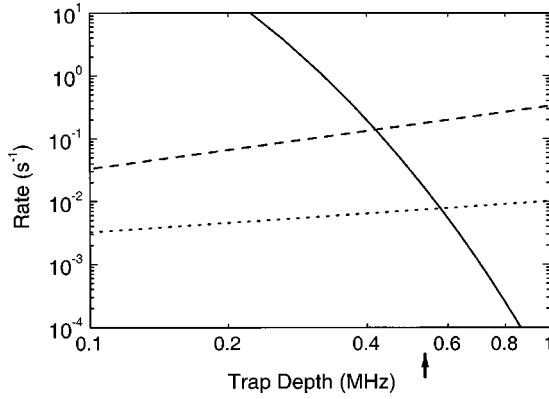
FIG. 2. Ground-state tunneling rate and scattering rate in a blue-detuned and a red-detuned dipole trap. The ground-state tunneling rate Γ is indicated by the solid line; the dotted and dashed lines indicate the photon scattering rate for a blue- and a red-detuned lattice, respectively, assuming the same lattice detuning. The arrow marks the operation point of our proposed configuration.

pressed to values below $\Delta\nu = 100$ nHz and $T^{-1} = 1$ s^{-1}, respectively.

To achieve shot-noise limited sensitivity for $N = 10^8$ atoms, a signal-to-noise ratio of $N^{1/2} = 10^4$ is necessary. Stability of both the detection and the Raman lasers is crucial at this level, as recently demonstrated in an atomic clock experiment with 6×10^5 cesium atoms, where the shot noise limit was attained [19]. If the same laser is used both for signal detection and for normalization, the influence of laser noise is greatly reduced. In this case we are only sensitive to noise near the frequency corresponding to the time interval between detection and normalization pulses, and 10^{-4} stability of the intensity in this frequency band can be achieved without much difficulty. The same 10^{-4} intensity stability is also required for the Raman lasers which generate the $\pi/2$ pulses for the state preparation.

For a specific calculation, we propose the geometry given in Fig. 1 and the following trap parameters which are chosen based on the discussion in Sec. V. The optical lattice is generated by a high-power, frequency-doubled single-mode neodimium-doped yttrium aluminum garnet (Nd:YAG) laser at a wavelength of $\lambda = 532$ nm. A frequency difference on the order of several MHz is applied between the three linearly polarized standing waves to ensure that the total light field is effectively linearly polarized throughout space. The lattice spacings in the principal lattice directions x, y, and z are $\lambda/2$, $\lambda/[2\cos(\theta/2)]$, and $\lambda/[2\sin(\theta/2)]$, respectively, where $\theta = 10°$ is the angle between two horizontal standing waves. The trap depth is then chosen to be $U_0 = h\,527$ kHz $= k_B 25\,\mu$K based on the trade-off between the photon scattering rate [20] and the atom tunneling rate between neighboring lattice sites that is discussed in Sec. III and also shown in Fig. 2. The trap vibration frequencies of $\omega_x = (2U_0 k_x^2/m)^{1/2} = 2\pi\,105$ kHz, $\omega_y = (4U_0 k_y^2/m)^{1/2} = 2\pi\,148$ kHz, and $\omega_z = (4U_0 k_z^2/m)^{1/2} = 2\pi\,13.0$ kHz along x, y, and z, respectively, correspond to Lamb–Dicke parameters $\eta_i = k_i x_{\mathrm{rms},i}$ of $\eta_x = 0.22$, $\eta_y = 0.18$, and $\eta_z = 0.055$. Here $\mathbf{k} = (k_x, k_y, k_z) = (2\pi/\lambda)[1, \cos(\theta/2), \sin(\theta/2)]$, is the

reciprocal lattice vector and $x_{\mathrm{rms},i} = (\hbar/2m\omega_i)^{1/2}$ is the rms spread of the ground-state wave function along the ith axis. The average intensity and ac Stark shift experienced by the atoms in the 3D vibrational ground state are 6.3 kW/cm^2 and 66.5 kHz, respectively. If the mean occupancy of lattice sites is $L = 1/200$, $N = 10^8$ atoms will be confined in a volume of only $V = NL\,(\lambda^3/8\sin\theta) = 2.2$ mm^3 at a bulk density of $D = N/V = 4.6 \times 10^{10}$ cm^{-3}.

III. COLLISION-INDUCED LEVEL SHIFTS AND DECOHERENCE

We begin our discussion of the proposed scheme with the issue of cold atom interactions. According to a theoretical calculation for Cs atoms in a superposition of $|3,\pm1\rangle$ states, the collision-induced relative energy shift between these states at a density of $D = 4.6 \times 10^{10}$ cm^{-3} and a temperature of 2.5 μK will be $\Delta P \nu_{\mathrm{coll}}$, where ΔP is the single-particle population difference between the $|3,1\rangle$ and $|3,-1\rangle$ states, and $\nu_{\mathrm{coll}} = 30$ mHz [21]. Fluctuations of the relative populations of these two states or of the density will therefore translate directly into an apparently fluctuating EDM signal. If we assume a similar interaction for a $|3,\pm2\rangle$ superposition, our target frequency resolution of $\Delta\nu = 100$ nHz would require a stability of the average density and population difference better than $\Delta P = \Delta\nu/\nu_{\mathrm{coll}} = 3 \times 10^{-6}$ upon static electric field $\mathbf{E_S}$ reversal, if the atoms were allowed to collide.

If individual atoms are isolated at separate sites of a 3D optical lattice, however, these collisional effects can be greatly suppressed. For the configuration described above, only $L = 1/200 = 0.5\%$ of the atoms will be loaded into doubly occupied lattice sites, and at these sites the high local density will lead to radiative collisional loss during optical cooling [22]. For atoms trapped in singly occupied lattice sites and cooled to the vibrational ground state, the collision rate is limited by the site-to-site tunneling rate, i.e., the width of the lowest vibrational energy band. Given a sinusoidal optical lattice potential, the equation of motion can be simplified and rewritten in terms of Mathieu functions [23]. The ith energy bandwidth can be obtained from its characteristic functions [23]. In our case, the ground-state tunneling rate Γ can be approximated as $\hbar\Gamma = 2^{9/2}\pi^{-1/2}U_0\eta\exp(-\eta^{-2})$ in the tight-binding regime [23], shown in Fig. 2. Because of the exponential dependence, tunneling occurs predominantly along the axis with the largest Lamb-Dicke parameter $\eta_x = 0.22$. For a lattice spacing D, the effective velocity is estimated classically as ΓD, and for the above parameters the collision rate is reduced by a factor of 10^6 compared to free atoms with the same kinetic energy and bulk density. The corresponding frequency shift is then $\Delta P \times 30$ nHz, which is negligible compared to our required $\Delta\nu = 100$ nHz frequency resolution as long as $\Delta P \ll 1$. It should be noted in this context that the Cs–Cs interaction parameters are now known to be different than previously assumed [24], and that the predictions of Ref. [21] may need further modification in light of the more recent collision results [24,25].

IV. ATOM–STATIC FIELD INTERACTION

The interaction between a cesium atom and the external static fields is given by

$$H_{\text{static}} = -\mu \cdot \mathbf{B}_S - R_{\text{Cs}} \mathbf{d_e} \cdot \mathbf{E_S} - \frac{1}{2} \alpha_{\text{dc}} \cdot E_s^2 - \mathbf{E_S^*} \cdot \overset{\leftrightarrow}{\mathbf{T}}_{\mathbf{dc}} \cdot \mathbf{E_S},$$

where the four terms on the right-hand side indicate the Zeeman effect, EDM effect, and scalar and tensor parts of the quadratic Stark effect. $\alpha_{\text{dc}}(\overset{\leftrightarrow}{T}_{\mathbf{dc}})$ is the scalar (tensor) part of the dc polarizability. Note that in our configuration both the static magnetic field $\mathbf{B}_S$ and the static electric field $\mathbf{E}_S$ are oriented along the z axis, so $|F, m_F\rangle$ remain approximate eigenstates.

A. Required magnetic field stability and comagnetometer

An external magnetic field $B_s = 7$ mG inducing an energy splitting of $-\mu \cdot \mathbf{B}_S = h10$ kHz between the $|3, \pm 2\rangle$ states defines the quantization axis and keeps the trapped atoms spin polarized during the measurements. Since the Zeeman effect dominates the energy splitting, stability of the magnetic field is a major concern. Furthermore, frequent reversal of the B_s field, necessary to suppress the related systematic error, could lead to hysteresis effects from the magnetic shielding and any ferromagnetic material near the experiment. Fluctuations of the field strength lead to a reduction of the fringe contrast while a systematic change associated with the $\mathbf{E}_S$ reversal mimics the EDM signal. The required frequency resolution of $\xi = 16 \, \mu\text{Hz}/\sqrt{\text{Hz}}$ and systematic error $\Delta \nu = 100$ nHz require that the fluctuations of the external magnetic field during the $T = 1$ s integration time are controlled to less than $\delta B = h \xi T^{1/2} / \mu = 11$ pG and that the systematic change in field strength be less than $\Delta B = h \Delta \nu / \mu = 80$ fG upon $\mathbf{E}_S$ field reversal.

A spatial field variation across the cloud below this level can be achieved by multiple magnetic shielding and magnetic coils to zero the stray field and field gradient [26]. The temporal fluctuations of $\mathbf{B}_S$ are dominated by the noise of the current source. During the $T = 1$ s integration time, the atoms are most sensitive to the noise in the 100–700 mHz band. A current supply with an integrated noise in this band providing a stability better than $\iota = 1$ ppb has been designed [27], which applied to our case yields a field variation of $<\iota B_s = 7$ pG, better than the required stability $\delta B = 11$ pG.

Systematic effects associated with the $\mathbf{E}_S$ and the $\mathbf{B}_S$ reversal include the hysteresis effect mentioned above and the leakage current from the electric field plates. The latter has long been considered the limiting systematic error of cell-type EDM experiments [28]. The idea of a ''comagnetometer,'' where auxiliary atoms with a small EDM are used to monitor the magnetic field, was first suggested in Ref. [8]. With this approach, a recent neutron EDM experiment reached a field sensitivity of 2 nG per shot [3]. In our proposal, rubidium atoms with a smaller enhancement factor can be loaded into the same optical lattice and used as a comagnetometer to monitor the magnetic field and eliminates the effects of systematic variation of $\mathbf{B}_S$ and the leakage current

[26]. Similar to cesium atoms, rubidium atoms can be optically cooled and trapped in the ground states of the 3D lattice sites where all rubidium atoms and cesium atoms are isolated from each other. We also expect a similar frequency sensitivity for the Ramsey interferometry of rubidium. Assuming the same measurement scheme is applied to $N_{\text{Rb}} = 10^8$ ^{87}Rb atoms in the upper hyperfine manifold $F = 2$, the long term drift can be corrected to $h\xi/2\mu = 5.5$ pG$/\sqrt{\text{Hz}}$ and the systematic field shift can be measured to an accuracy of $h\Delta\nu/2\mu = 40$ fG. Note that the larger magnetic moment of the ^{87}Rb state $|2, \pm 2\rangle$ compared to the Cs state $|3, \pm 2\rangle$ increases the magnetic field sensitivity by a factor of 2. Further discussion of the rubidium comagnetometer is given in Sec. V D.

B. Calibration of electric field reversal

In addition to the EDM effect, the static electric field $E_s = 10^7$ V/m also induces a quadratic Stark shift [29,30] on Cs atoms in the $|F = 3, m_F\rangle$ state given by

$$\delta f = -\frac{1}{2} E_s^2 \left(\alpha - \frac{9}{7} \alpha_{10} + \frac{3m_F^2 - 12}{28} \alpha_{12} \right) \Big/ h$$

$$\approx -500 \, \text{MHz} - 19.6 m_F^2 \, \text{Hz},$$

where $\alpha/h = 1.00 \times 10^{-5}$ Hz/(V/m)^2 is the dc polarizability of the Cs ground state averaged over hyperfine levels. $\alpha_{10}/h = 1.99 \times 10^{-10}$ Hz/(V/m)^2 and $\alpha_{12}/h = 3.65 \times 10^{-12}$ Hz/(V/m)^2 are the additional corrections due to the hyperfine contact interaction and the spin-dipolar interaction, respectively [29,30]. (The small contribution from the Cs nuclear electric quadrupole moment is negligible here.)

In a previous EDM experiment involving polarization precession [28], the m_F^2-dependent tensor shift gives rise to severe dephasing and systematic error when the static field reverses imperfectly. Our proposed measurement based on the energy splitting between $|3, \pm 2\rangle$, however, is not affected by the tensor shift. Furthermore, this energy shift provides a handle to calibrate the field strength and to reduce field gradients and imperfections of field reversal.

According to the recent measurement in Ref. [30], a field $E_s = 10^7$ V/m can cause a frequency shift of $\kappa = 2\pi 22.7$ kHz on the $|3, 0\rangle$ to $|4, 0\rangle$ clock transition. The energy resolution of $\xi = 16 \, \mu\text{Hz}/\sqrt{\text{Hz}}$ of our experiment will theoretically allow the field and its reversal to be calibrated with a fractional accuracy of $2\pi\xi/\kappa < 10^{-9}/\sqrt{\text{Hz}}$. The $T = 1$ s coherence time can also be used to correct the field gradient to achieve a fractional variation in $\mathbf{E}_S$ of less than $(T\kappa)^{-1} \sim 7 \times 10^{-6}$ over the atom cloud. Since these theoretical limits are much better than those that have been practically realized [28], we will conservatively assume a $\Delta E_s/E_s = 10^{-3}$ accuracy in field reversal and a $\mathbf{E}_S$ field variation of $\nabla E_s V^{1/3} = 10^{-3} E_s$ across the with volume V of the sample for the following discussion.

V. SUPPRESSION OF DETRIMENTAL LASER-INDUCED EFFECTS

Next we consider the interaction between the atoms and the far-detuned trapping light. In a blue-detuned trap, the

TABLE I. Various interaction effects in the proposed EDM experiment. Energy shifts are calculated perturbatively for cesium atoms in the $F=3$ manifold in the vibrational ground state of the 3D optical lattice. $\hat{\mathbf{f}} \equiv \mathbf{F}/F$, $\hat{\mathbf{f}}^2 = \hat{\mathbf{f}} \cdot \hat{\mathbf{f}}$, $\hat{f}_z = \hat{\mathbf{f}} \cdot \hat{\mathbf{z}}$, and $\hat{f}_\perp = \hat{\mathbf{f}} \cdot \hat{\mathbf{x}}$ or $\hat{\mathbf{f}} \cdot \hat{\mathbf{y}}$. The static magnetic and electric fields are $B_S = 7$ mG, $E_S = 10^7$ V/m, and the beam configuration is that shown in Fig. 1. The energy scale column gives the frequency shifts for atoms localized in the vibrational ground state with the chosen configuration. Note that only terms with $\hat{f}_z$ dependence can give rise to systematic errors.

Interaction	Hamiltonian	Atomic polarization dependence	Energy scale	$|3, \pm 2\rangle$ level splitting	systematic	Reference
EDM	$-R_{Cs} d_e \hat{\mathbf{f}} \cdot \mathbf{E_S}$	$\hat{\mathbf{f}} \cdot \mathbf{E_S}$	$< 11 \, \mu$Hz $\hat{f}_z$	$< 11 \, \mu$Hz		
Zeeman shift	$-\boldsymbol{\mu} \cdot \mathbf{B_S}$	$\hat{\mathbf{f}} \cdot \mathbf{B_S}$	-10 kHz $\hat{f}_z$	-10 kHz	field instability	
dc polarization	$(-\mathbf{d} \cdot \mathbf{E_S})(-\mathbf{d} \cdot \mathbf{E_S})$	1	-500 MHz	0	0	[34]
Quadratic dc Stark shift	$(-\mathbf{d} \cdot \mathbf{E_S})(-\mathbf{d} \cdot \mathbf{E_S})$	$\mathbf{E_S^*} \cdot [\hat{\mathbf{f}}^2 - \mathrm{Tr}(\hat{\mathbf{f}}^2)] \cdot \mathbf{E_S}$	-310 Hz $\hat{f}_z \cdot \hat{f}_z$	0	0	[30]
Scalar light shift	$(-\mathbf{d} \cdot \mathbf{E_L^*})(-\mathbf{d} \cdot \mathbf{E_L})$	1	67 kHz	0	0	[20]
m_F-dependent light shift	$(-\mathbf{d} \cdot \mathbf{E_L^*})(-\mathbf{d} \cdot \mathbf{E_L})$	$\hat{\mathbf{f}} \cdot \mathbf{k}$	-10 mHz $\hat{f}_z +$ 0.2 Hz $\hat{f}_\perp$	-10 mHz	polarization instability	[9,33]
m_F^2-dependent light shift	$(-\mathbf{d} \cdot \mathbf{E_L^*})(-\mathbf{d} \cdot \mathbf{E_L})$	$\mathbf{E_L^*} \cdot [\hat{\mathbf{f}}^2 - \mathrm{Tr}(\hat{\mathbf{f}}^2)] \cdot \mathbf{E_L}$	-4 mHz $\hat{f}_z \cdot \hat{f}_z$ -4 mHz $\hat{f}_\perp \cdot \hat{f}_\perp$	0	0	[9,10]
Field gradient effect		$\hat{\mathbf{f}} \cdot \mathbf{B_S}$, $\hat{\mathbf{f}} \cdot \mathbf{k}$	40 nHz $\hat{f}_z$	40 nHz	70 pHz	
Third-order effect	$(-\mathbf{d} \cdot \mathbf{E_L^*})(-\mathbf{d} \cdot \mathbf{E_S})$ $(-\boldsymbol{\mu} \cdot \mathbf{B_L})$, $(-\mathbf{d} \cdot \mathbf{E_L^*})(-\mathbf{d} \cdot \mathbf{E_S})$ $\left(-\dfrac{1}{6} \mathbf{Q} \cdot \nabla \mathbf{E_L}\right)$	$(\mathbf{E_L^*} \cdot \mathbf{E_S})(\hat{\mathbf{f}} \cdot \mathbf{B_L})$, $(\mathbf{B_L^*} \cdot \mathbf{E_S})(\hat{\mathbf{f}} \cdot \mathbf{E_L})$	-80 nHz $\hat{f}_z -$ $80 \, \mu$Hz $\hat{f}_\perp$	-80 nHz	-80 nHz	[38]
Higher-order effect			< 10 nHz $\hat{f}$	< 10 nHz	< 10 nHz	

atoms are attracted towards the low-intensity regions. Although the intensity of the trapping light vanishes at the potential minima (nodes) of the lattice, the finite spatial spread of the vibrational ground-state wave function leads to an average intensity $\langle I \rangle$ experienced by atoms of $\langle I \rangle = (\eta_x^2/3 + 2\eta_y^2/3 + 2\eta_z^2/3) I_{peak}$, where I_{peak} is the peak intensity. For the beam parameters defined above, the average intensity experienced by the atoms is reduced by a factor $I_{peak}/\langle I \rangle = 24$ compared to a red-detuned lattice with the same beam intensity. This helps to suppress the systematic effects associated with various atom-light interactions, which in most cases are proportional to the intensity experienced by the atoms.

The interaction between the atoms and the laser field can be written as a multipole expansion of the electric and magnetic interactions, $H_{int} = -\mathbf{d} \cdot \mathbf{E_L} - \boldsymbol{\mu} \cdot \mathbf{B_L} - 1/6 \mathbf{Q} \cdot \nabla \mathbf{E} + \cdots$, where $\mathbf{E_L}$ and $\mathbf{B_L}$ are the laser electric and magnetic fields, $\mathbf{d}$ and $\boldsymbol{\mu}$ denote the atomic electric and magnetic dipole moments, respectively, and $\mathbf{Q}$ denotes the electric quadrupole moment. For the EDM measurement we are concerned with the relative level shifts of the states $F=3$, $m_F = \pm 2$ arising from these interactions, and with the broadening of these levels associated with spatial inhomogeneities, temporal fluctuations, and coupling to other magnetic sublevels. Table I lists the various interactions that warrant consideration and the coupling factors that enter in a perturbative treatment. The corresponding energy scale and the angular dependence are also shown. The effects can be classified into three cat-

egories: photon scattering, light shifts, and light-induced coupling between energy levels.

A. Photon scattering

Scattering of photons from the far detuned light field results in heating by Rayleigh scattering, which preserves the internal atomic state, and spin relaxation by Raman scattering, which changes the internal state [20]. For the above beam parameters, these rates are estimated to be $\Gamma_{Ray} = (140 \text{ s})^{-1}$ and $\Gamma_{Ram} = (10^5 \text{ s})^{-1}$, respectively, where only the strongest coupling to the nearby $6P$ and $7P$ states has been included [31]. In the measurement time of $T=1$ s, only $\Gamma_{Ray} T = 0.7\%$ of the atoms scattered one photon and only $\Gamma_{Ram} T = 0.001\%$ are transferred to other magnetic sublevels. While the Raman scattering leads to loss of fringe contrast, the Rayleigh scattering merely heats the atoms but preserves the relative phase between the states $|3,2\rangle$ and $|3,-2\rangle$ as long as the laser field has no preferred helicity along the quantization axis [32].

B. ac Stark shift

Various coherent processes due to laser fields have been considered in the literature and are summarized in Table I. We estimate the various interactions based on the configuration in Fig. 1, where the field orientations are designed to minimize the level shifts, and the bias field direction (z axis)

is defined as the quantization axis. The atom–laser interaction Hamiltonian can be written as

$$H_{\mathrm{laser}} = -\frac{1}{2}\alpha_{\mathrm{ac}}\cdot E_L^2 - \beta\mathbf{f}\cdot\mathbf{k}E_L^2 - \mathbf{E}_\mathbf{L}^*\cdot\overset{\leftrightarrow}{\mathbf{T}}_{\mathbf{ac}}\cdot\mathbf{E_L},$$

where $\alpha_{\mathrm{ac}}(\overset{\leftrightarrow}{\mathbf{T}}_{\mathbf{ac}})$ is the scalar (tensor) part of the ac polarizability, $\mathbf{k}$ is the wave vector of the laser, and β is a constant which depends on laser detuning and polarization. The various ac Stark effects induce light shifts ΔE that can be written according to their dependence on m_F: $\Delta E = A_0 + A_1 m_F + A_2 m_F^2$. The m_F-even terms A_0, A_2 do not directly affect our measurement, which involves the energy splitting between the $|3,2\rangle$ and the $|3,-2\rangle$ states. The m_F-odd term A_1 is of prime importance since the linear Stark effect resulting from electron's EDM is also m_F odd. In addition, these light shift effects can induce coupling between m_F levels.

The most significant m_F-odd level shift is the light shift associated with a residual circularly polarized component of the light field. Based on our configuration, the frequency shift is calculated to be $\hat{\mathbf{k}}\cdot\hat{\mathbf{f}}A_L$ for a fully circularly polarized lattice [33], where the caret indicates a dimensionless unit vector and $A_L = 2.7$ kHz. To suppress this shift, the trapping beams are chosen to be linearly polarized, and interferences between beams from different directions are avoided by shifting the relative frequency by several MHz. This insures averaging on a time scale below 1 μs, which is much shorter than the atomic vibration period. Furthermore, since the lattice beams are oriented nearly perpendicular to the quantization axis, any imperfection in their linear polarization yields predominantly coupling to other magnetic sublevels rather than an m_F-odd light shift. Assuming a polarization impurity of $\varepsilon_p \approx 10^{-5}$, the linear level shift can be reduced to $f_l = 4\varepsilon_p A_L \sin\theta/2 \approx 10$ mHz, mainly coming from the four beams in the y-z plane. Although this is not in itself a systematic effect, it puts a stringent limit of $\Delta\nu/f_l = 10^{-5}$ on the required stability of the light intensity and polarization upon $\mathbf{E_S}$ reversal.

An additional consideration is the coupling between different magnetic sublevels. For example, the residual circularly polarized light also couples the neighboring m_F states with a Rabi frequency Ω of $\Omega/2\pi = 6\varepsilon_p A_L \approx 0.2$ Hz. Coupling between $|F,m_F\rangle$ states reduces the contrast of the interference fringes and induces decoherence if Ω is spatially varying. These detrimental effects can be suppressed with a large magnetic field $\mathbf{B_S}$ which strongly splits the levels and reduces the coupling to $\Gamma_1 = \Omega^2/\omega_L$, where Ω is assumed to be small compared to an assumed Larmor frequency ω_L of $\omega_L/2\pi = \mu B_s/h = 10$ kHz. The coupling between sublevels then gives a negligible decoherence rate of $\Gamma_1 = (1000\,\text{s})^{-1}$.

The m_F^2-dependent shift A_2 is dominated by the tensor light shift characterized by the effective quadrupole tensor operator $\overset{\leftrightarrow}{\mathbf{T}} \propto \hat{\mathbf{f}}\hat{\mathbf{f}} - \mathrm{Tr}(\hat{\mathbf{f}}^2)$ [9] and results in a frequency shift of $f_t = \hat{\mathbf{E}}_\mathbf{s}^*\cdot\hat{\mathbf{f}}\hat{\mathbf{f}}\cdot\hat{\mathbf{E}}\cdot\hat{\mathbf{E}}_\mathbf{s}$ 4 mHz for our configuration. This level shift does not affect our measurement which involves only the relative energy splitting between $|3,2\rangle$ and $|3,-2\rangle$.

C. Displacement of atoms due to field gradients

Although scalar level shifts are not themselves systematic effects, their spatial inhomogeneity can result in a static force and lead to a displacement of the atoms. Any change of this displacement associated with an imperfect reversal of $\mathbf{E_S}$ therefore represents a systematic error if the Zeeman splitting or tensor light shift is not spatially uniform. Given a static electric field $E_s = 10^7$ V/m, the large dc polarizability of Cs atoms leads to a scalar energy shift $\Delta_E/h = -500$ MHz [34] which, when combined with the field gradient ∇E_s, results in a displacement of the atoms given by $d \approx h\Delta_E(\nabla E_s/E_s)(k^2 U_0)^{-1}$, where k is the beam wave vector and U_0 the lattice trap depth. For an imperfection of the field reversal ΔE_s, the displacement changes by $\delta d = d\Delta E_s/E_s$. Following the discussion in Sec. IV B, we assume $\nabla E_s = 10^{-3}E_s/D_e$, where $D_e \sim 1$ cm is the spacing between the field plates, and $\Delta E_s = 10^{-3}E_s$. Due to the weak confinement, this shift is largest along the z axis with $d \sim 0.1$ nm and $\delta d \sim 0.1$ pm. We consider below two leading-order systematic frequency shifts which are associated with the inhomogeneity of the magnetic field and of the tensor light shift.

A magnetic-field gradient leads to a direct change of the Zeeman energy splitting between the states $|3,2\rangle$ and $|3,-2\rangle$ when the atoms are displaced. We assume that the gradients can be canceled experimentally by minimizing the linewidth of rf transitions, for example, between m_F levels. Given a coherence time T of 1 s and an atomic cloud size of $D_A = 2$ mm such a measurement will have a sensitivity to magnetic-field gradients of order $|\partial B_s/\partial z| \lesssim \mu^{-1}(\hbar/T)/D_A = 0.7$ μG/cm, and should allow the gradients to be canceled to this level. In the presence of such a gradient, the residual systematic shift associated with the displacement of the atoms upon E_s reversal is $\sim\mu|\partial B_s/\partial z|\delta d = h\,10$ pHz, much smaller than the projected $\Delta\nu = 100$ nHz resolution. Note, however, that in a conventional focused dipole trap with a similar trap depth but much weaker confinement, the displacement due to field gradient is given by $d = h\Delta_E(\nabla E_s/E_s)(K^2 U_0)^{-1}$, where $K = 2\pi/D_A$, and the systematic error amounts to ~ 1 μHz for the same cloud size D_A, which is intolerable [35]. This emphasizes the importance of very strong confinement when trapped atoms are used for EDM measurements [36].

A similar effect will occur if the atoms experience a different tensor light shift between the $|3,2\rangle$ and $|3,-2\rangle$ states upon $\mathbf{E_S}$ reversal due to a change in their field gradient-induced displacement. According to the previous section, this frequency shift f_L can be formulated as $f_L = f_l d^2/z_{\mathrm{rms}}^2$, where d is the small displacement of the atom position and $z_{\mathrm{rms}} = \eta_z/k_z = 54$ nm is the rms ground state spread in the z direction. Given $d = 0.1$ nm and $\delta d = 0.1$ pm, the systematic shift is $\delta f_L = f_l 2d\,\delta d/z_{\mathrm{rms}}^2 \sim 70$ pHz, which is also negligible.

D. Estimation and suppression of higher-order interactions

A third-order interference effect was first identified in Ref. [10] as a possible systematic error for EDM experiments

using optically trapped atoms. It represents the dipole energy $\langle \tilde{g} | -\mathbf{d} \cdot \mathbf{E_S} | \tilde{g} \rangle$ of a ground-state atom which is perturbed by the laser field through both the electric dipole interaction $E1$ and the magnetic dipole (or electric quadrupole) interaction $M1(E2)$. In a perturbative treatment, this expression describes a third-order energy shift induced by both laser fields and the static $\mathbf{E_S}$ field, and can be written as

$$\langle H_3 \rangle = \sum_{i,j} \frac{\langle g | E1 | i \rangle \langle i | -\mathbf{d} \cdot \mathbf{E_S} | j \rangle \langle j | M1(E2) | g \rangle}{(E_{gi} - \hbar \omega_L)(E_{gj} - \hbar \omega_L)},$$

where the sum is over all possible intermediate states i and j with energies E_{gi} and E_{gj}. The contributions from all possible third-order terms are considered in [10] and the dominant effect here gives $\langle H_3 \rangle = h \gamma_1 (\hat{\mathbf{E}}_\mathbf{L}^* \cdot \hat{\mathbf{E}}_\mathbf{S})(\hat{\mathbf{B}}_\mathbf{L} \cdot \hat{\mathbf{f}}) + h \gamma_2 (\hat{\mathbf{B}}_\mathbf{L}^* \cdot \hat{\mathbf{E}}_\mathbf{S})(\hat{\mathbf{E}}_\mathbf{L} \cdot \hat{\mathbf{f}})$, where the unit vectors indicate the vector dependence of this effect and $\gamma_1 = 7$ mHz and $\gamma_2 = 9$ mHz [37]. The energy shift is proportional to $\mathbf{E_S} m_F$ and can therefore constitute an important systematic error. Two-fold cancellation of this systematic error is obtained for our field geometry. First, all laser polarizations E_L are chosen perpendicular to both $\mathbf{E_S}$ and $\hat{\mathbf{f}}$. Second, for atoms trapped at the nodes of the standing waves, the couplings $\langle | (\hat{\mathbf{E}}_\mathbf{L}^* \cdot \hat{\mathbf{E}}_\mathbf{S})(\hat{\mathbf{B}}_\mathbf{L} \cdot \hat{\mathbf{f}}) | \rangle$ and $\langle | (\hat{\mathbf{B}}_\mathbf{L}^* \cdot \hat{\mathbf{E}}_\mathbf{S})(\hat{\mathbf{E}}_\mathbf{L} \cdot \hat{\mathbf{f}}) | \rangle$ are forbidden because the total interaction has odd spatial parity about the potential minimum. ($\mathbf{E_L}$ fields are odd about the nodes and $\mathbf{B_L}$ fields even if the intensities of the counterpropagating laser beams are balanced). Assuming an intensity imbalance of $\varepsilon_i \approx 10^{-3}$, and an alignment uncertainty of $\varepsilon_a = \hat{\mathbf{E}}_\mathbf{L} \cdot \hat{\mathbf{E}}_\mathbf{S} \approx \hat{\mathbf{E}}_\mathbf{L} \cdot \hat{\mathbf{f}} \approx 10^{-4}$, we expect the effect to be reduced to $6 \varepsilon_i \varepsilon_a (\gamma_1 + \gamma_2) \approx h \, 10$ nHz, where the factor 6 reflects the number of beams in the 3D lattice. This systematic effect on the Rb atoms, the comagnetometer, is as large as $h \, 80$ nHz [38], which is close to our proposed frequency resolution. Calibration of this systematic effect can be achieved by measuring the dependence of this shift on laser intensity.

Coupling by H_3 to another magnetic sublevel can also lead to decoherence. This coupling is not suppressed by precise beam imbalance when the final state is a different vibrational state with different spatial parity. Symbolically, given the initial external vibrational quantum number n, the coupling is estimated as $\langle n \pm 1 | H_3 | n \rangle \approx 6 \, \varepsilon_a h (\gamma_1 + \gamma_2) = h \, 10 \, \mu$Hz. At the large vibrational level spacings considered here this coupling is reduced to a negligible level.

In general, higher-order polarizabilities should also be considered in the presence of external static fields ($\mathbf{E_S}$ and $\mathbf{B_S}$) and laser fields ($\mathbf{E_L}$ and $\mathbf{B_L}$). We shall limit our consideration here to the possible systematics which carry the $E_s \hat{\mathbf{f}}$ dependence and imitate the EDM effect. More explicitly, the relevant interaction should be odd in powers of $\mathbf{E_S}$ and $\hat{\mathbf{f}}$. Given that an energy shift operator must have even parity ($E1$ transition is odd, $M1$ even, and $E2$ even), the next order effects satisfying these criteria are given by the fifth-order polarizabilities which involve the following field combinations: $\mathbf{E_S E_L B_L E_S E_S}$, $\mathbf{E_S E_L B_L B_S B_S}$, $\mathbf{E_S E_L B_L E_L E_L}$, or $\mathbf{E_S E_L B_L B_L B_L}$. All of these terms can be factored into the

product of the third-order shift H_3 and the quadratic dc (ac) Stark(Zeeman) shift H_2. Their strength can be estimated as

$$\langle H_5 \rangle = \sum_i \frac{\langle g | H_3 | i \rangle \langle i | H_2 | g \rangle}{\Delta E_{gi}},$$

where the dominant terms come from the coupling to higher center-of-mass vibrational states. As estimated above, the coupling $\langle i | H_3 | g \rangle$ is typically $h \, 10 \, \mu$Hz, and the coupling from various possible H_2 is dominated by the vector light shift which was estimated in Sec. V B as $\langle i | H_2 | g \rangle = h 0.2$ Hz. This results in $\langle H_5 \rangle / h < 1$ nHz(< 10 nHz for rubidium [38]), where the small vibration frequency 13 kHz in the z direction is used. Although this value is considerably lower than our proposed $\Delta \nu = 100$ nHz sensitivity, a rigorous calculation might be necessary in the future.

VI. CONCLUSION

In summary, we have proposed a measurement of the linear Stark shift in the cesium ground state caused by an electron EDM. Our method is based on trapping atoms in a far-detuned 3D optical lattice. A linearly polarized trichromatic lattice is used to avoid the vector light shift associated with a circularly polarized component. For atoms thus strongly confined, velocity-induced dephasing, inhomogeneous broadening effects, collisional frequency shifts, and field gradient-induced displacements are dramatically reduced. Furthermore, rubidium atoms simultaneously trapped in the same volume can act as an effective comagnetometer to monitor the drifts and the systematic effects associated with the magnetic field. We have discussed various systematic effects associated with atom-field and atom-atom interactions, and presented experimental schemes to suppress them. These systematic effects for our configuration are summarized in Table I. The m_F-odd energy shift (terms with $\hat{\mathbf{f}}_z$) is dominated by the residual circularly polarized component of the laser beams, and needs to be controlled to $\Delta \nu = 100$ nHz upon field reversal, corresponding to a stringent stability of 10^{-5} of the polarization and intensity. Another major systematic effect is the third-order polarizability which can be suppressed to values of 10 nHz for Cs atoms and 80 nHz for Rb atoms. Higher-order processes are estimated to contribute less than 10 nHz and further investigation of them is necessary. If all these criteria are met, our proposed measurement should approach a frequency resolution of $\Delta \nu = 100$ nHz, which corresponds to a 100 times higher sensitivity than the current upper bound for the electron's EDM.

[1] S. M. Barr, Int. J. Mod. Phys. A **8**, 209 (1993).

[2] W. R. Johnson, D. S. Guo, M. Idrees, and J. Sapirstein, Phys. Rev. A **34**, 1043 (1986).

[3] P. G. Harris, C. A. Baker, K. Green, P. Iaydjiev, S. Ivanov, D. J. R. May, J. M. Pendlebury, D. Shiers, K. F. Smith, M. van der Grinten, and P. Geltenbort, Phys. Rev. Lett. **82**, 904 (1999).

[4] J. P. Jacobs, W. M. Klipstein, S. K. Lamoreaux, B. R. Heckel, and E. N. Fortson, Phys. Rev. A **52**, 3521 (1995).

[5] E. S. Commins, S. B. Ross, D. DeMille, and B. C. Regan, Phys. Rev. A **50**, 2960 (1994).

[6] P. G. H. Sandars and Lipworth, Phys. Rev. Lett. **13**, 718 (1964).

[7] N. Davidson, H. J. Lee, C. S. Adams, M. Kasevich, and S. Chu, Phys. Rev. Lett. **74**, 1311 (1995).

[8] N. F. Ramsey, Acta Phys. Hung. **55**, 117 (1984).

[9] W. Happer and B. S. Mathur, Phys. Rev. **163**, 12 (1967).

[10] M. V. Romalis and E. N. Fortson, Phys. Rev. A **59**, 4547 (1999).

[11] K. Gibble and S. Chu, Phys. Rev. Lett. **70**, 1771 (1993).

[12] S. E. Hamann, D. L. Haycock, G. Klose, P. H. Pax, I. H. Deutsch, and P. S. Jessen, Phys. Rev. Lett. **80**, 4149 (1998); V. Vuletic, C. Chin, A. J. Kerman, and S. Chu, *ibid.* **81**, 5768 (1998); H. Perrin, A. Kuhn, I. Bouchoule, and C. Salomon, Europhys. Lett. **42**, 395 (1998); A. J. Kerman, V. Vuletic, C. Chin, and S. Chu, Phys. Rev. Lett. **84**, 439 (2000); D.-J. Han, S. Wolf, S. Oliver, C. McCormick, M. T. DePue, and D. S. Weiss, *ibid.* **85**, 724 (2000).

[13] P. G. H. Sandars, Phys. Lett. **14**, 194 (1965).

[14] Z. W. Liu and H. P. Kelly, Phys. Rev. A **45**, R4210 (1992).

[15] A. C. Hartley, E. Lindroth, and A.-M. Martensson-Pendrill, J. Phys. B **23**, 3417 (1990).

[16] N. Ramsey, *Molecular Beams* (Clarendon, Oxford, 1985).

[17] J. Vanier and C. Audoin, *The Quantum Physics of Atomic Frequency Standards* (Hilger, Bristol, 1989).

[18] Recently, a multiple-level interferometry scheme has been reported which approaches 79% of the Heisenberg limit $(32\pi^2 NtT)^{-1/2}$ for Cs atoms in the $F=4$ hyperfine manifold [G. Xu and D. J. Heinzen, Phys. Rev. A **59**, R922 (1999)]. However, when a strong electric field is applied, the quadratic Stark shift results in unequal spacings between m_F levels and could lead to strong reduction of fringe contrast or even systematic errors. On the other hand, our proposed scheme is immune to this quadratic Stark effect which does not change the energy spacing between the $|3,2\rangle$ and the $|3,-2\rangle$ state.

[19] G. Santarelli, Ph. Laurent, P. Lemonde, A. Clairon, A. G. Mann, S. Chang, A. N. Luiten, and C. Salomon, Phys. Rev. Lett. **82**, 4619 (1999).

[20] R. Loudon, *The Quantum Theory of Light* (Clarendon, Oxford, 1983).

[21] M. Bijlsma, B. J. Verhaar, and D. J. Heinzen, Phys. Rev. A **49**, R4285 (1994).

[22] M. T. DePue, C. McCormick, S. L. Winoto, S. Oliver, and D. S. Weiss, Phys. Lett. **82**, 2262 (1999).

[23] N. W. McLachlan, *Theory and Application of Mathieu Function* (Dover, New York, 1964); J. Meixner and F. W. Schäfke, *Mathieusche Funktionen und Sphäroidfunktionen* (Springer-Verlag, Berlin, 1954).

[24] C. Chin, V. Vuletic, A. J. Kerman, and S. Chu, Phys. Rev. Lett. **85**, 2717 (2000); P. J. Leo, C. J. Williams, and P. S. Julienne, *ibid.* **85**, 2721 (2000).

[25] J. Söding, D. Guéry-Odelin, P. Desbiolles, G. Ferrari, and J. Dalibard, Phys. Rev. Lett. **80**, 1869 (1998); D. Guéry-Odelin, J. Söding, P. Desbiolles, and J. Dalibard, Opt. Express **2**, 323 (1998); P. J. Leo, E. Tiesinga, P. S. Julienne, D. K. Walter, S. Kadlecek, and T. G. Walker, Phys. Rev. Lett. **81**, 1389 (1998); V. Vuletic, A. J. Kerman, C. Chin, and S. Chu, *ibid.* **82**, 1406 (1999); V. Vuletic, C. Chin, A. J. Kerman, and S. Chu, *ibid.* **83**, 943 (1999); V. Vuletic, A. J. Kerman, C. Chin, and S. Chu, in *Proceedings of the 14th International Conference on Laser Spectroscopy*, edited by R. Blatt, J. Eschner, D. Leibfrried, and F. Schmidt-Kaler (World Scientific, Singapore, 1999).

[26] I. B. Khriplovich and S. K. Lamoreaux, *CP Violation Without Strangeness* (Springer, New York, 1997).

[27] C. Ciofi, R. Giannetti, V. Dattilo, and B. Neri, in *Proceedings of the 14th IEEE Instrumentation and Measurement Technology Conference, Ottawa, Canada, 1997* (IEEE, New York, 1997).

[28] S. A. Murthy, D. Krause, Z. L. Li, and L. R. Hunter, Phys. Rev. Lett. **63**, 965 (1989).

[29] J. P. Carrico, A. Adler, M. R. Bakers, S. Legowski, E. Lipworth, P. G. H. Sandars, T. S. Stein, and M. C. Weisskopf, Phys. Rev. **170**, 64 (1968).

[30] E. Simon, P. Laurent, and A. Clairon, Phys. Rev. A **57**, 436 (1998).

[31] The contribution from the $7P$ and $8P$ states is considerable much smaller than from the $6P$ states. This is because the oscillator strength of the $7P$ states is $\sim 10^{-2}$ weaker and $8P$ states $\sim 10^{-3}$.

[32] W. D. Philips and C. I. Westbrook, Phys. Rev. Lett. **78**, 2676 (1997).

[33] Contributions from the $6P$ and $7P$ states are included, and both rotating and counter-rotating components are considered.

[34] T. M. Miller and B. Bederson, Adv. At. Mol. Phys. **13**, 1 (1977).

[35] L. Hunter (private communication).

[36] The gravitational force also has the same effect and shifts the equilibrium position. For the optical lattices we consider, this effect is negligible.

[37] M. Romalis (private communication).

[38] For Rb atoms, $\gamma_1 = -0.1$ Hz and $\gamma_2 = -0.02$ Hz,; see M. Romalis (private communication).